JOC The Journal of Organic Chemistry

Article

Synthesis of Fullerene–Fluorene Dyads through the Platinum-Catalyzed Reactions of [60]Fullerene with 9-Ethynyl-9H-fluoren-9-yl Carboxylates

Michio Yamada, Mayu Takizawa, Yoko Nukatani, Mitsuaki Suzuki, and Yutaka Maeda

J. Org. Chem., **Just Accepted Manuscript** • DOI: 10.1021/acs.joc.9b00932 • Publication Date (Web): 17 Jun 2019

Just Accepted

is published by the American Chemical Society. 1155 Sixteenth Street N.W., Washington, DC 20036

Synthesis of Fullerene–Fluorene Dyads through the Platinum-Catalyzed Reactions of [60]Fullerene with 9-Ethynyl-9*H*-fluoren-9-yl Carboxylates

Michio Yamada,*,† Mayu Takizawa,† Yoko Nukatani,† Mitsuaki Suzuki,‡ and Yutaka Maeda†

†Department of Chemistry, Tokyo Gakugei University, Koganei, Tokyo 184-8501, Japan

‡Department of Chemistry, Josai University, Sakado, Saitama 350-0295, Japan

ABSTRACT

The single-step regio- and stereoselective platinum-catalyzed reactions of [60]fullerene with a series of 9-ethynyl-9*H*-fluoren-9-yl carboxylates afforded fullerene–fluorene dyads in their [2+2] cycloaddition forms. The presented reactions represent the first examples of the use of easily accessible fluorenyl carboxylates as fluorenylideneallene precursors. In addition, the single-crystal X-ray structure of one of the dyads reveals a distorted cyclobutane ring. Furthermore, the dyad forms a layered structure with close-packed arrays of C_{60} spheres in its crystals.

INTRODUCTION

Allenes are recognized as valuable precursors to a number of products in modern synthetic chemistry owing to their abilities to undergo a variety of skeletal transformations.[1] In particular, allene unsaturation, which is spread over three carbon atoms, provides powerful access to carbo- and heterocycles through tandem or multistep reactions.[2] In addition, allenes have been used in a wide range of asymmetric catalytic and natural-product syntheses because they

provide axially chiral scaffolds when appropriately substituted.[3,4] Notably, allenes can be used to functionalize fullerene, which has been a fascinating research topic in materials chemistry.[5,6,7,8] The chemical reactivities, as well as the electronic and optical properties of allenes can be tuned through the incorporation of substituents. Fluorenylideneallenes have been reported to be highly reactive and to easily dimerize to form isomeric mixtures of cyclobutanes even at low temperature.[9,10] Therefore, fluorenylideneallenes have rarely been explored for synthetic chemistry applications. Mcglinchey et al. developed a new synthetic route to tetracenes through the dimerization of fluorenylideneallenes,[9b] while Alcarazo and coworkers reported the synthesis of organic frustrated Lewis pairs by the reactions of fluorenylideneallenes with *N*-heterocyclic carbenes.[11]

Recently, we demonstrated that transition-metal-catalyzed reactions of [60]fullerene (C_{60}) and propargylic esters yielded formal [2+2] cycloadducts (alkylidenecyclobutane-annulated fullerenes)[12] and [4+2] cycloadducts (cyclohexene-annulated fullerenes) in reasonable yields.[8] We found that the choice of metal catalyst had a profound effect on the outcome of the reaction; formal [2+2] cycloadducts were dominantly formed when CuCl was used, and [4+2] cycloadducts were dominantly formed when $AgOCOCF_3$ was loaded as the catalyst. In that case, the formal [2+2] cycloadditions are likely to involve the formation of allene intermediates through 6-*endo*-*dig* cyclization reactions aided by the transition-metal catalyst. This achievement motivated us to explore the reactivities of fluorenylideneallenes with fullerenes by examining the reactions of C_{60} with 9-ethynyl-9*H*-fluoren-9-yl carboxylates. We envisaged that treatment of these carboxylates with a transition metal catalyst would readily generate fluorenylideneallene intermediates in-situ, and that these intermediates would be trapped by C_{60} to yield novel fullerene–fluorene dyads in one step. In related work, Galloni, Gatto, and their coworkers reported the synthesis of

two fullerene–fluorene dyads with different position linkage of the fluorene group by the Prato reaction, and revealed that the ground and excited state properties of the molecules were modulated by changing the position of the fluorene chromophore.[13] The formation of [4+2] cycloadducts is prohibited in the proposed scheme because the introduction of the fluorenylidene structure excludes the formation of 1,3-dienyl ester intermediates that facilitate the formal [4+2] cycloaddition with C_{60}. In this work, we found that the platinum-catalyzed reactions of C_{60} with the above-mentioned carboxylates afforded the corresponding fullerene–fluorene dyads in their [2+2] cycloaddition forms in reasonable yields and with high regio- and stereoselectivities, as described below.

RESULTS AND DISCUSSION

The syntheses of the 9-ethynyl-9*H*-fluoren-9-yl carboxylates **2** and the fullerene–fluorene dyads **3** are summarized in Scheme 1 and Table 1. These carboxylates were appended with different substituents (R^1) on the acetylenic terminal in order to investigate the substituent dependence of these reactions, while long alkyl chains were incorporated into **2a**–**2c** for solubility reasons. In a typical procedure, a mixture of C_{60} and **2** (6.0 equiv. based on C_{60}) in toluene was treated with a catalytic amount of $PtCl_2$ (0.3 equiv. based on C_{60}) at 80 ºC for 4–6 h. The reaction was monitored by TLC and HPLC. The dyads were purified and isolated by silica-gel flash chromatography and, if necessary, subsequent preparative HPLC using a Buckyprep column. The HPLC profiles of the reaction mixtures provided contrasting features compared to those of **2a**–**2c** (Figure S4). In the reaction of C_{60} with **2a**, two fullerene derivatives, ***Z*-3a** and ***E*-3a**, were obtained in yields of 3% and 25%, respectively (Table 1, entry 1). Notably, the reactions of C_{60} with **2b** or **2c** gave ***Z*-3b** (45%) or ***Z*-3c** (12%) as the sole dyad (Table 1, entries 3 and 5). Increasing the amount of **2c** (12 equiv. based on C_{60}) in the reaction with C_{60} had no beneficial effect on the yield of ***Z*-3c** (Table

1, entry 6). In addition to dyads **3**, a complex mixture of non-fullerene products was predominantly formed in the reaction of C_{60} with **2b** or **2c** (see Figure S4). Although the separation and full characterization of such non-fullerene products were difficult, they are likely to be isomeric mixtures of cyclobutanes formed by dimerization of in-situ generated fluorenylideneallene intermediates (see Figure 1). The formation of these dimers was suggested by the MALDI-TOF mass spectrometry (see Figure S8). Using CuCl as a catalyst instead of $PtCl_2$ in the reactions of C_{60} with **2a–2c** afforded none of the desired product; both the carboxylates and C_{60} were scarcely consumed after heating at 80 ºC for 4 h (Table 1, entries 2, 4, and 7).

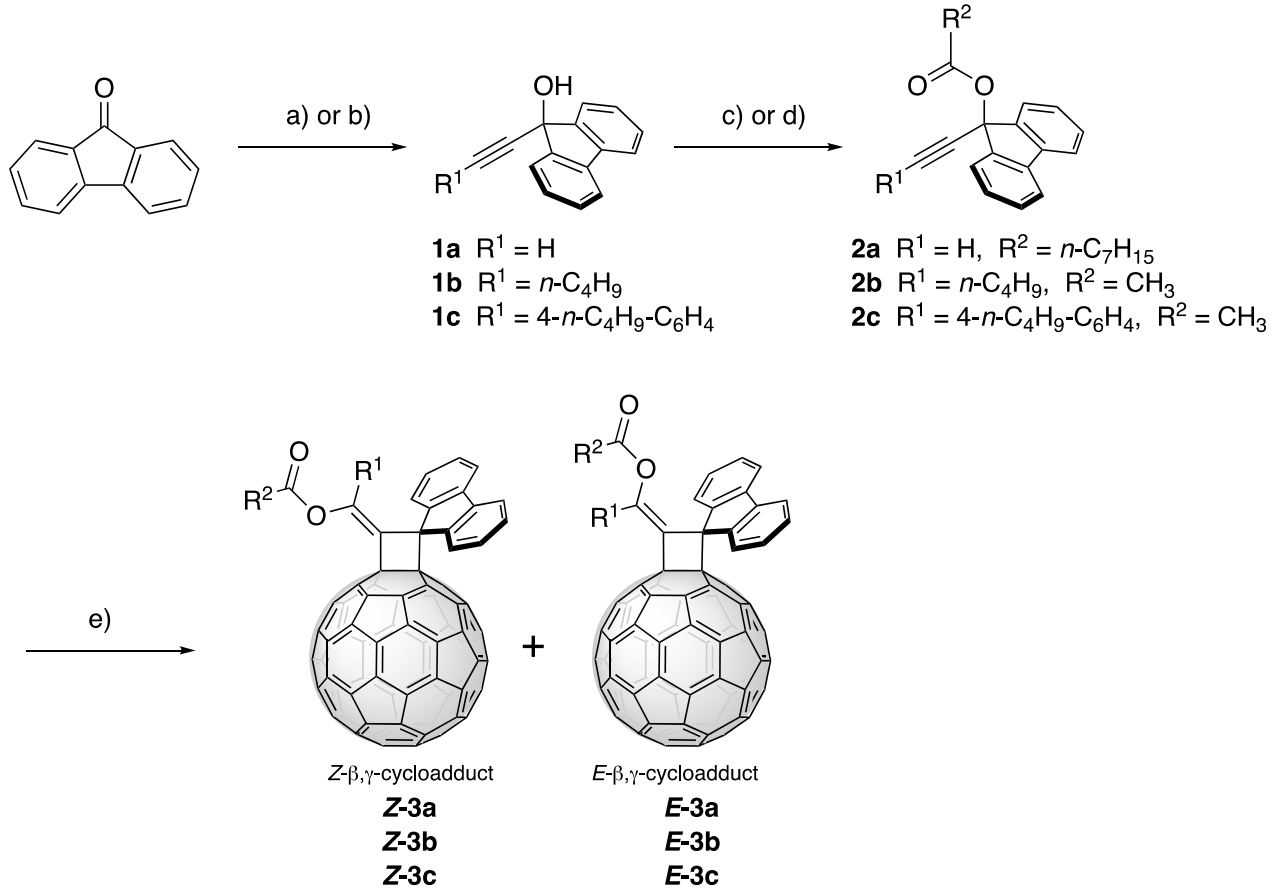

Scheme 1. Synthesis of 9-ethynyl-9*H*-fluoren-9-yl carboxylates 2a–2c and fullerene–fluorene dyads *E*/*Z*-3. a) i) *n*-BuLi, trimethylsilylacetylene, Et_2O, ii) K_2CO_3, THF, MeOH; 52% (1a). b) *n*-BuLi, 1-hexyne or 1-*n*-butyl-4-ethynylbenzene, THF, then NH_4Cl/H_2O; 79% (1b), 93% (1c). c) *n*-octanoyl chloride, *N*,*N*-dimethyl-4-

aminopyridine (DMAP), Et_3N, CH_2Cl_2; 97% (2a). d) Ac_2O, pyridine, K_2CO_3; 99% (2b), 87% (2c). e) C_{60}, catalyst, toluene. Yields are summarized in Table 1.

Table 1. Transition-Metal-Catalyzed Reaction of C_{60} with 2

Entry	**2**	Catalyst	Molar ratio[a]	Yield[b] of ***Z*-3**	Yield[b] of ***E*-3**
1	**2a**	$PtCl_2$	6 : 1 : 0.3	3% (3%)	25%(29%)
2	**2a**	CuCl	6 : 1 : 0.3	0%	0%
3	**2b**	$PtCl_2$	6 : 1 : 0.3	45% (67%)	0%
4	**2b**	CuCl	6 : 1 : 0.3	0%	0%
5	**2c**	$PtCl_2$	6 : 1 : 0.3	12% (67%)	0%
6	**2c**	$PtCl_2$	12 : 1 : 0.3	11% (61%)	0%
7	**2c**	CuCl	6 : 1 : 0.3	0%	0%

[a]Molar ratio refers to [**2**]:[C_{60}]:[catalyst].

[b]Yield of isolated product. The values in parentheses are conversion yields based on the amount of C_{60} consumed.

Dyads ***Z*-3a**, ***E*-3a**, ***Z*-3b**, and ***Z*-3c** were characterized by MALDI-TOF mass spectrometry as well as by absorption and IR spectroscopy. The MALDI-TOF mass spectrum of each dyad exhibits the corresponding parent peak (see Figure S7). However, the relative intensity of the parent peak was very weak in each case; instead, a strong fragment peak due to the C_{60} cage was observed, which corresponds to the loss of the entire addend. These results suggest that

the retro-cycloaddition takes place easily during mass spectrometry. The absorption spectra of dyads ***Z*-3a**, ***E*-3a**, ***Z*-3b**, and ***Z*-3c** exhibit features characteristic of [6,6]-closed addition forms (see Figure S9). The ^{1}H NMR spectra of ***Z*-3a** and ***E*-3a** reveal that both dyads have C_s symmetry based on the pairwise equivalency of the fluorene aromatic protons, which indicates the formation of the β,γ-cycloaddition product. In this context, we note that α,β-cycloaddition leads to C_1 symmetric products (i.e., α,β-cycloadduct **4**) as shown in Figure 1. The vinylcarbenoid addition to form a cyclopropanated derivative is also a possible pathway (see Scheme 2). The cyclopropane structure, which must have C_1 symmetry, was also excluded based on the molecular symmetry. The ^{13}C NMR spectra of both ***Z*-3a** and ***E*-3a** show 30 peaks in the ~137–153 ppm range, which are due to the sp^2 carbon atoms of the C_{60} skeleton and the fluorene core, and are consistent with structures of C_s symmetry.

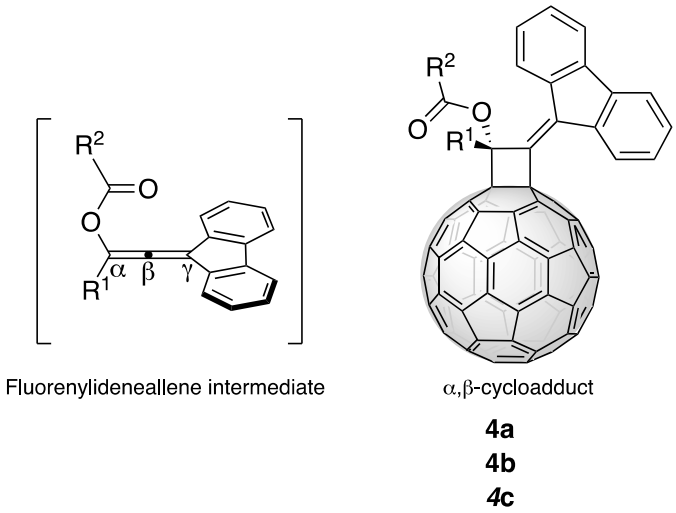

Figure 1. Structures of the fluorenylideneallene intermediates and the α,β-cycloadducts.

The ^{1}H NMR chemical shifts of the fluorene skeletons of ***Z*-3a** and ***E*-3a** are almost identical. On the other hand, the chemical shifts of the olefinic protons in ***Z*-3a** (7.66 ppm) and ***E*-3a** (8.10 ppm) are quite different; this difference is most likely due to the distance between the olefinic proton atom and the fullerene surface. In the *E*-β,γ-cycloadduct, the olefinic proton is more affected by the ring current of the fullerene surface because of its close proximity. On the

other hand, the olefinic proton in the *Z*-β,γ-cycloadduct is more distant from the fullerene surface. Therefore, ***Z*-3a** and ***E*-3a** are assigned to be the Z-β,γ- and *E*-β,γ-cycloadducts, respectively. The observed ^{1}H NMR chemical shifts are also in good agreement with the chemical shifts calculated for model compounds ***Z*-3d** and ***E*-3d** (R^1 = H, R^2 = CH_3) at the GIAO[14]-B3LYP/6-31G(d) level of theory using the B3LYP/6-31G(d) optimized geometries (see Figures S13 and S14).[15] In addition, the ***E*-3a** geometry was assigned on the basis of NOESY NMR spectroscopy, in which correlations between the octanoyl group and the fluorene moiety are clearly observed (see Figure S34). Similarly, the ^{1}H and ^{13}C NMR spectra of ***Z*-3b** and ***Z*-3c** are also consistent with C_s symmetry. In addition, the geometrical assignments of both ***Z*-3b** and ***Z*-3c** were provided by NOESY spectroscopy in which the required correlations between the butyl or butylphenyl groups and the fluorene moieties are clearly observed.

The detailed structure of ***Z*-3b** was revealed by single-crystal X-ray diffractometry (see Figure 2), which confirmed the *Z*-β,γ-cycloaddition form of ***Z*-3b**. Black plate crystals of the compound suitable for data collection were obtained by gradual diffusion of *n*-hexane into a solution of ***Z*-3b** in CS_2/*n*-hexane. The ORTEP drawing shown in Figure 2 represent the first example of an X-ray crystallographic study of an alkylidenecyclobutane-annulated fullerene. In fact, known examples of crystallographically identified C_{60}-based [2+2] cycloadducts are limited.[16] The alkylidenecyclobutane moiety is distorted: C1–C2 (1.609 Å), C2–C61 (1.521 Å), C61–C62 (1.528 Å), C1–C62 (1.616 Å), C61–C75 (1.322 Å), C2-C61-C62 (95.80º), C61-C62-C1 (87.30º), C62-C1-C2 (89.06º), and C1-C2-C61 (87.80º). The distortion seems to arise through angle strain at the C61 sp^2 hybridized carbon. The fullerene C(sp^3)–C(sp^3) bond length in ***Z*-3b** (i.e., C1–C2 in Figure 2a) is similar to those reported for methanofullerenes (1.57–1.61Å)[17] and Diels–Alder adducts (1.59–1.62 Å).[18] The packing structure reveals that ***Z*-3b** forms layers parallel to

the *ab* plane in which layers of C_{60} moieties alternate with layers of addends along the *c* axis. In fact, the plane of the crystal plates is in accordance with the *ab* plane (see Figure S1). Within a layer, each C_{60} moiety is in close contact (~3.36 Å) with six other C_{60} moieties, which constitutes a close-packed array of spheres. Such molecular packing of two-dimensional crystalline ordering may be valuable in bulk heterojunction polymer solar cell applications.[19]

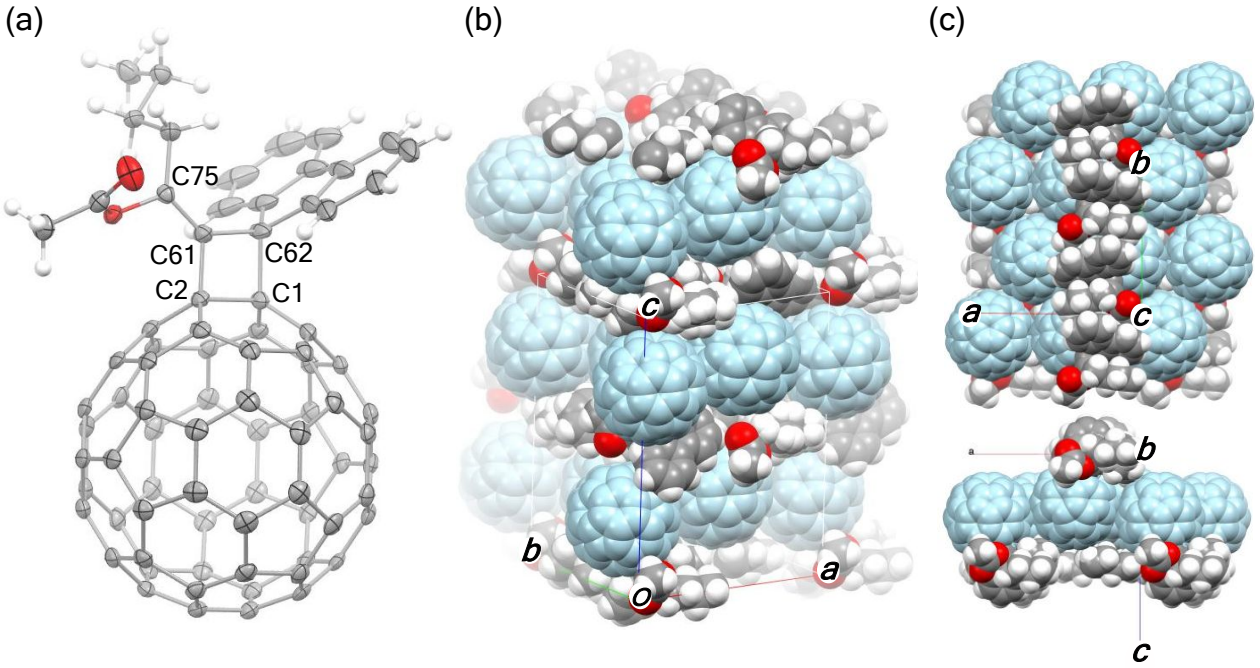

Figure 2. (a) ORTEP drawing of *Z*-3b with thermal ellipsoids shown at the 50% probability level; the disordered *n*-butyl moiety is omitted for clarity. (b) Packing structure in which the fullerene cages are highlighted in light blue. (c) Two orthogonal views of a single layer of fullerene spheres.

To assess the thermal stabilities of these dyads, they were heated at elevated temperatures and monitored for changes by HPLC. When the dyads were heated at 80 ºC for 1 h in toluene, they did not decompose (Figure S11). Retro-cycloaddition dominated at 110 ºC and C_{60} was the major product after 1 h, indicating that the decomposition pathway dominates in all cases (Figure S12). As for ***Z*-3a**, a small amount of ***E*-3a** was observed in addition to C_{60} produced by the retro-cycloaddition process. Similarly, a small amount of ***Z*-3a** was formed in addition to C_{60} when

a toluene solution of ***E*-3a** was heated at 110 ºC. As for ***Z*-3b** and ***Z*-3c**, heating at 110 ºC for 1 h resulted in retro-cycloaddition to give C_{60}, while no other isomers, such as ***E*-3b** or ***E*-3c**, were detected. In this context, we conclude that the products decompose negligibly during the presented $PtCl_2$-catalyzed reactions of C_{60} with **2a–2c**.

To gain insights into the selectivities, we computed the relative energies of possible structurally isomeric formal [2+2] cycloadducts, as summarized in Figure 3. The α,β-cycloadduct was calculated to be thermodynamically most stable when R^1 = H, while the *Z*- and *E*-β,γ-cycloadducts are respectively 5.61 and 5.92 kcal mol^{-1} higher in energy than the α,β-cycloadduct. Given that the corresponding α,β-cycloadducts were not observed experimentally, it is reasonable to conclude that the β,γ-cycloaddition is a thermodynamically disfavored but kinetically favored process when R^1 = H. Meanwhile, the energy difference between the α,β-cycloadduct and the *E*/*Z*-β,γ-cycloadducts is very small (< 0.50 kcal mol^{-1}) when R^1 = CH_3. Furthermore, the *E*/*Z*-β,γ-cycloadducts are more stable than the α,β-cycloadduct when R^1 = Ph; notably, the *Z*-β,γ-cycloadduct is 4.19 kcal mol^{-1} lower in energy than the α,β-cycloadduct. These results suggest that substituent R^1 plays an important role in determining the relative energies of these isomers; an alkyl or an aryl group leads to β,γ-cycloaddition thermodynamically favored over α,β-cycloaddition. The calculations also suggest that the *Z*-isomers are more stable than the *E*-isomers, regardless of the substituent on the β,γ-cycloadduct. On the one hand, the mechanism of the intramolecular [2+2] cycloaddition has been an important topic in allene chemistry, in which most examples have been explained by a stepwise diradical mechanism.[11] It is also noteworthy that transition metals can catalyze the [2+2] cycloadditions of allenes.[20] Further information on the reaction mechanism involved in the formation of the [2+2] cycloadducts presented herein is lacking; however, we deem that the preferential formation of the β,γ-cycloadducts rather than the α,β-cycloadducts may be governed by

the favorable localization of either spin or charge over the fluorene moieties in the corresponding singly-bonded intermediates (see Figure S3).[21,22] In related work, Ryu et al. reported that $PtCl_2$ catalyzes the reactions of propargylic esters bearing phenylacetylene moieties but devoid of fluorene moieties (i.e., 1,3-diphenylprop-2-yn-1-yl pivalate and 1-phenylhept-1-yn-3-yl pivalate) to give the corresponding α,β-cycloadducts.[7] Therefore, we conclude that the reactivities of fluorenylideneallenes toward C_{60} is different from those of other allenol esters. The preferential transformation of the *E*-β,γ-cycloadduct into the *Z*-β,γ-cycloadduct in the reaction of C_{60} with **2a** is possibly due to steric repulsion between the acetoxy group and the fullerene surface.

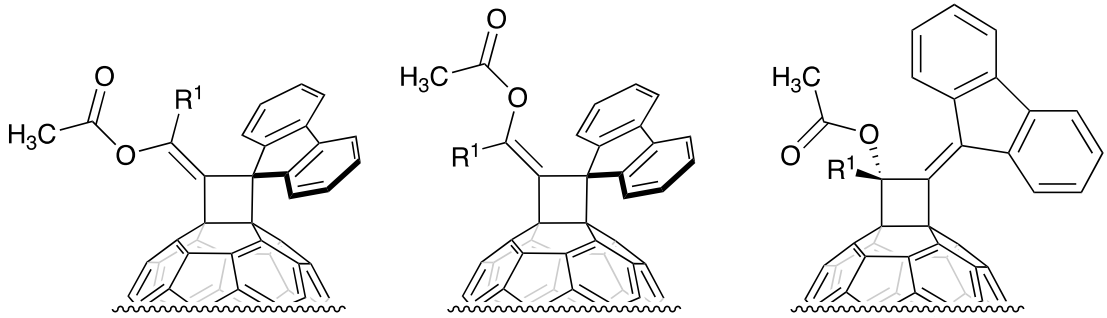

	Z-β,γ-cycloadduct	*E*-β,γ-cycloadduct	α,β-cycloadduct
R^1 = H	0.00	+0.31	–5.61
R^1 = CH_3	0.00	+0.67	+0.46
R^1 = Ph	0.00	+0.45	+4.19

Figure 3. Schematic structures and B3LYP/6-31G(d)+ZPVE-calculated relative energies (kcal mol^{-1}) of possible structural isomers of the formal [2+2] cycloadduct, where R^2 = CH_3.

It is also noteworthy that the presented reactivities of the 9-ethynyl-9*H*-fluoren-9-yl carboxylates toward C_{60} and furans are different. Ohe et al. reported that 9-ethynyl-9*H*-fluoren-9-yl carboxylates react with furans in the presence of $PtCl_2$ in toluene at 50 ºC to give 9-acyloxy-9-ethynylfluorene derivatives in excellent yields.[23] In that case, $PtCl_2$ activates the alkyne to generate an electrophilic vinylcarbenenoid[24] through a 5-*exo*-*dig*-mode 1,2-acyloxy migration, and the resulting vinylcarbenoid promotes the subsequent ring-opening of the furan. These contrastive results suggest

that the in-situ generated vinylcarbenenoids and fluorenylideneallenes are interconvertible in such systems and that these interconversions take place through double 1,2-acyloxy migrations and/or combinations of 6-*endo-dig*-mode 1,3-acyloxy migrations and 5-*exo-dig*-mode 1,2-acyloxy migrations, as shown in Scheme 2. Known examples of metal carbene complexes that exhibit reactivity toward C_{60} are limited.[25,26]

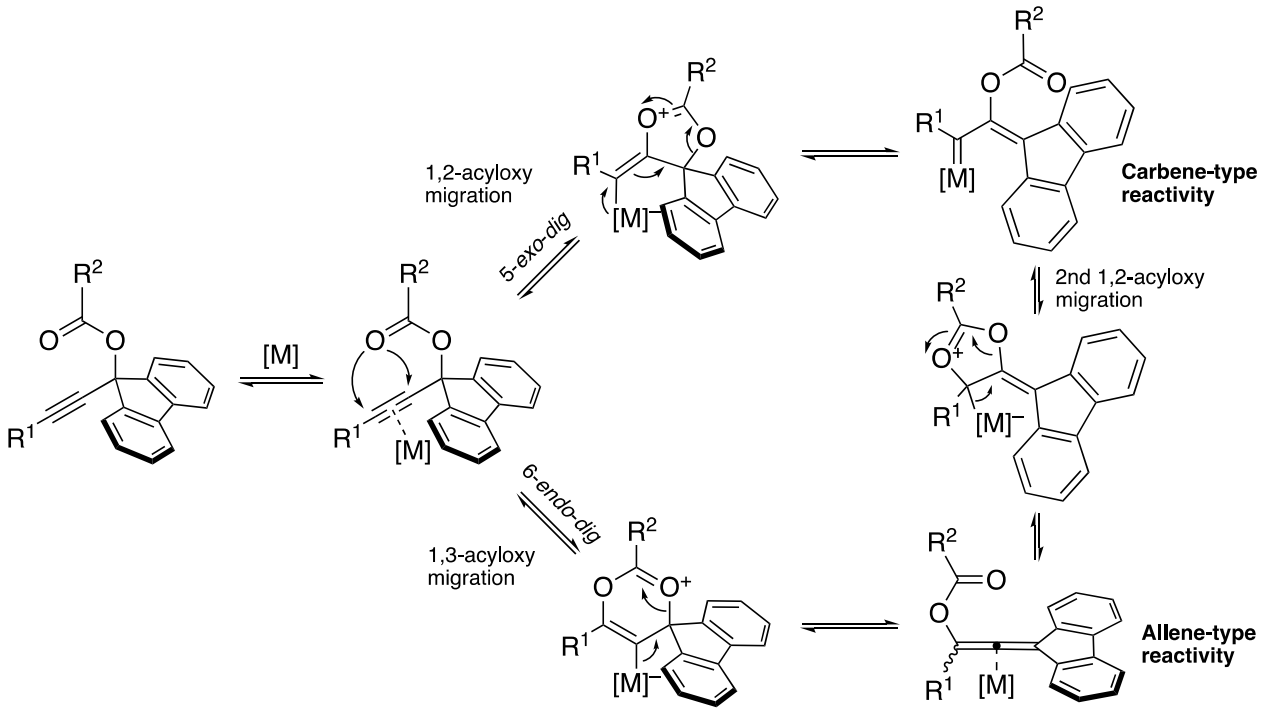

Scheme 2. Proposed mechanism for the skeletal transformation of a 9-ethynyl-9*H*-fluoren-9-yl carboxylate.

Electronic properties were electrochemically characterized in 1,2-dichlorobenzene (1,2-DCB) containing 0.1 M $(n\text{-Bu})_4NPF_6$ (see Figure S15). The reduction potentials of dyads **3** and related compounds, such as α,β-cycloadducts **4e** and **4f** as well as C_{60}[27] reported previously, are summarized in Table 2. The fullerene–fluorene dyads exhibit similar reversible reduction properties to those of other alkylidenecyclobutane-annulated fullerenes devoid of fluorene moieties,[8] suggesting that electronic interactions between the fullerene cores and the fluorene moieties are very weak.

Table 2. Reduction Potentials[a] (V vs. Fc/Fc$^+$) of Dyads 3 and Related Compounds

Compound	$^{red}E_1$	$^{red}E_2$
***E*-3a**	–1.25	–1.62
***Z*-3b**	–1.20	–1.59
***Z*-3c**	–1.17	–1.56
4e[b]	–1.20	–1.58
4f[b]	–1.23	–1.63
C_{60} [c]	–1.13	–1.50

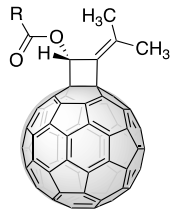

4e (R = CH_3)
4f (R = Ph)

[a]Determined using CV. [b]Ref. 8. [c]Ref.27.

CONCLUSIONS

In conclusion, we functionalized C_{60} with 9-ethynyl-9*H*-fluoren-9-yl carboxylates through platinum catalysis. These transformations represent the first examples of the use of these carboxylates as fluorenylideneallene precursors. β,γ-Cycloaddition proceeded smoothly to afford novel fullerene–fluorene dyads through formal [2+2] cycloadditions involving in-situ generated fluorenylideneallene intermediates. Acetylene-capped carboxylates **2b** and **2c** displayed uniform regio- and stereoselectivities in their cycloadditions to C_{60}. The structure of dyad ***Z*-3b** was unambiguously elucidated by X-ray crystallography, which revealed that the adducts formed layered structures containing close-packed arrays of C_{60} spheres. This study demonstrated that these carboxylates undergo a variety of skeletal transformations that serve as powerful methods for the functionalization of fullerenes, yielding new structural motifs such as fullerene–polyarene dyads. We expect that the presented reaction is applicable to other polyarenes, such as

indenofluorenes and sumanene.

EXPERIMENTAL SECTION

Reagents and solvents were purchased as reagent grade from commercial suppliers and used as received unless otherwise noted. Diethyl ether (Et_2O) and dichloromethane (CH_2Cl_2) were distilled over CaH_2. 1,2-Dichlorobenzene (1,2-DCB) was freshly distilled from CaH_2. Dehydrated tetrahydrofuran (THF) and toluene were purchased as Super plus grade from Kanto Kagaku and purified with a Glass Contour Solvent Dispensing System (Nikko Hansen & Co., Ltd.). All reactions were performed under an inert atmosphere by applying a positive pressure of argon unless otherwise stated. A personal organic synthesizer equipped with aliminum heating block units (ChemiStation PPV; EYELA) was used for reactions that require heating. When basification of silica gel was required for TLC analysis and column chromatography, the following amine-pretreatment was conducted prior to use: Silica gel 60 (particle size 0.040–0.050 mm, Kanto Chemical) or TLC plates (aluminum sheets coated with silica gel 60 F_{254} obtained from Merck) was immersed in *n*-hexane containing ca. 10vol% triethylamine and stand at room temperature over night. The amine-treated silica gel was packed in a column and washed with eluents for separation, or, the amine-treated TLC plates were taken out and was air-dried before use. Analytical high-performance column chromatography (HPLC) was run on a JASCO chromNAVI system equipped with a JASCO LC-Net II interface, a JASCO PU-2080 pump, a JASCO UV-2075plus UV-detector (330 nm) and a Buckyprep column (Nacalai Tesque; 40ºC in a column oven JASCO CO-2060plus) at flow rate of 1.0 mL min^{-1} with eluent of toluene unless otherwise stated. Preparative HPLC was performed using a chromatograph (LC-918; Japan Analytical Industry Co.) that was monitored using UV absorption at 330 nm. 1D and 2D NMR spectra were measured on a JEOL JNM-ECX400P spectrometer (400 MHz)

at room temperature unless otherwise stated. Chemical shifts δ are given in ppm relative to tetramethylsilane (TMS) and were referenced to internal TMS or residual non-deuterated solvent for ^{1}H and ^{13}C NMR spectra. Infrared spectra (IR) were recorded on a JASCO FT/IR4100 spectrometer equipped with a diamond ATR unit. Absorption spectra were recorded on a JASCO V670 spectrophotometer. MALDI-TOF mass spectra were measured on a Bruker Daltonics autoflex III smartbeam with 1,1,4,4-tetraphenylbuta-1,3-diene (TPB) as the matrix. Isotope distribution patterns were simulated using ChemCalc.[28] Electrochemical measurements were performed using an ALS electrochemical analyzer (model 630DT; BAS). A platinum disc and a platinum wire were used as the working electrode and the counter electrode, respectively. The reference electrode was a saturated calomel reference electrode (SCE). Analytes were dissolved in 1,2-DCB with $(n\text{-Bu})_4NPF_6$ (0.1 M). They were deaerated using freeze–pump–thaw cycles under reduced pressures. The measurement settings were as follows: scan rate = 20 mV s^{-1} for cyclic voltammetry (CV) measurements and pulse amplitude = 50 mV, pulse width = 200 msec, pulse period = 500 msec for differential pulse voltammetry (DPV) measurements. All potentials are referenced to the ferrocene/ferrocenium couple (Fc/Fc^{+}) as the standard. DFT calculations including zero-point vibration energy (ZPVE) correction were performed using *Gaussian 09* (Rev. D.01)[29] at the B3LYP/-31G(d)[30] level of theory.

Synthesis of Substrates

9-Ethynyl-9*H*-fluoren-9-ol (1a). The title compound **1a** was prepared according to a literature procedure.[31] Trimethylsilylacetylene (1.3 mL, 9.4 mmol) was dissolved in Et_2O (10 mL) in an oven-dried two-necked round bottom flask. The solution was cooled to –10 ºC and *n*-BuLi (1.6 M in *n*-hexane, 8.0 mL, 12.8 mmol) was added dropwise using a syringe, after which the solution was stirred for 1 h. 9*H*-Fluoren-9-one (1.99 g, 11.0 mmol) was

dissolved in Et_2O (15 mL) in a separate flask and cooled to –10 ºC. The 9*H*-fluoren-9-one solution was then added to the trimethylsilylacetylene/*n*-BuLi solution by syringe. The mixture was warmed to room temperature and stirred overnight, after which it was diluted with water (30 mL) and extracted with Et_2O (3 × 20 mL). The combined organic layers were dried over $MgSO_4$. The solution was concentrated under reduced pressure and the residue was recrystallized from CH_2Cl_2/*n*-hexane to afford crude 9-(trimethylsilyl)ethynyl-9*H*-fluoren-9-ol (2.17 g) as pale yellow crystals. The crude mixture (2.17 g) and K_2CO_3 (6.51 g, 47.1 mmol) were dissolved in a mixture of THF (35 mL) and methanol (35 mL) and stirred overnight at room temperature. Water (20 mL) was added to the mixture, after which was extracted with EtOAc (2 × 30 mL). The combined organic layers were dried over $MgSO_4$ and the solvent was removed under reduced pressure. The residue was purified by silica-gel flash chromatography (SiO_2; EtOAc/*n*-hexane 1:3) to afford **1a** (1.17 g, 52%). White solid; R_f = 0.28 (SiO_2; EtOAc/*n*-hexane 1:3); ^{1}H NMR (400 MHz, $CDCl_3$): δ 2.48 (s, 3H; CH_3), 2.62 (brs, 1H; O*H*), 7.36 (dd, *J* = 7.6, 1.2 Hz, 2H; Ar-*H*), 7.41 (dd, *J* = 7.6, 1.2 Hz, 2H; Ar-*H*), 7.60–7.64 (m, 2H; Ar-*H*), 7.69–7.73 (m, 2H; Ar-*H*) ppm; ^{13}C{^{1}H} NMR (100 MHz, $CDCl_3$): δ 71.5, 74.5, 83.9, 120.2, 124.3, 128.6, 129.8, 139.1, 146.6 ppm. The NMR data are in accord with the literature values.

9-(Hex-1-yn-1-yl)-9*H*-fluoren-9-ol (1b). The title compound **1b** was prepared according to a literature procedure.[32] 1-Hexyne (1.3 mL, 11.4 mmol) was dissolved in THF (40 mL) in an oven-dried two-necked round bottom flask. The solution was cooled to –78 ºC and *n*-BuLi (1.6 M in *n*-hexane, 7.8 mL, 12.0 mmol) was added dropwise using a syringe. The solution was stirred for 0.5 h. To the flask was added 9*H*-fluoren-9-one (1.50 g, 8.35 mmol) in THF (10 mL) dropwise by syringe. The mixture was warmed to room temperature and stirred overnight, after which it was quenched with saturated aqueous NH_4Cl (280 mL) and extracted with EtOAc (3 × 30 mL). The combined organic

layers were washed with saturated aqueous NH_4Cl (30 mL) and brine (30 mL), and dried over $MgSO_4$. The solvent was removed under reduced pressure and the residue was purified by silica-gel flash chromatography (SiO_2; EtOAc/*n*-hexane 1:6) to afford **1b** (1.74 g, 79%). Yellow oil; R_f = 0.23 (SiO_2; EtOAc/*n*-hexane 1:6); ^{1}H NMR (400 MHz, $CDCl_3$): δ 0.88 (t, *J* = 7.2 Hz, 3H; C*H*$_3$), 1.32–1.43 (m, 2H; C*H*$_2$), 1.43–1.53 (m, 2H; C*H*$_2$), 2.21 (t, *J* = 7.2 Hz, 2H), 2.49 (brs, 1H; O*H*), 7.34 (dd, *J* = 7.6, 1.2 Hz, 2H; Ar-*H*), 7.38 (dd, *J* = 7.6, 1.2 Hz, 2H; Ar-*H*), 7.59–7.63 (m, 2H; Ar-*H*), 7.67–7.71 (m, 2H; Ar-*H*) ppm; ^{13}C{^{1}H} NMR (100 MHz, $CDCl_3$): δ 13.7, 18.7, 22.1, 30.7, 75.1, 80.0, 84.5, 120.3, 124.3, 128.6, 129.6, 139.1, 147.8 ppm. The NMR data are in accord with the literature values.

9-((4-*n*-Butylphenyl)ethynyl)-9*H*-fluoren-9-ol (1c). 1-*n*-Butyl-4-ethynylbenzene (2.0 mL, 11.4 mmol) was dissolved in THF (40 mL) in an oven-dried two-necked round bottom flask. The solution was cooled to –78 ºC and *n*-BuLi (1.6 M in *n*-hexane, 7.8 mL, 12.0 mmol) was added dropwise using a syringe, after which the solution was stirred for 0.5 h. To the flask was added 9*H*-fluoren-9-one (1.51 g, 8.37 mmol) in THF (10 mL) dropwise by syringe. The mixture was warmed to room temperature and stirred overnight, after which it was quenched with saturated aqueous NH_4Cl (60 mL) and extracted with EtOAc (3 × 20 mL). The combined organic layers were washed with brine (30 mL) and dried over Na_2SO_4. The solvent was removed under reduced pressure and the residue was purified by silica-gel flash chromatography (SiO_2; EtOAc/*n*-hexane 1:4) to afford **1c** (2.65 g, 93%). Viscous pale yellow solid; R_f = 0.30 (SiO_2; EtOAc/*n*-hexane 1:4); m.p. 73–74ºC; ^{1}H NMR (400 MHz, $CDCl_3$): δ 0.93 (t, *J* = 7.4 Hz, 3H; C*H*$_3$), 1.34 (sext, *J* = 7.4 Hz, 2H; C*H*$_2$); 1.58 (quint, *J* = 7.4 Hz, 2H; C*H*$_2$), 2.59 (t, *J* = 7.4 Hz, 2H; C*H*$_2$), 2.75 (brs, 1H; O*H*), 7.10 (AA'BB', *J* = 8.0 Hz, 2H; Ar-*H*), 7.34–7.45 (m, 6H; Ar-*H*), 7.64 (d, *J* = 7.2 Hz; Ar-*H*), 7.79 (d, *J* = 7.2 Hz; Ar-*H*) ppm; ^{13}C{^{1}H} NMR (100 MHz, $CDCl_3$) δ 14.0 (*C*H$_3$), 22.3 (C*H*$_2$), 33.3 (C*H*$_2$), 35.5 (C*H*$_2$), 75.2, 83.4,

88.4, 119.5, 120.2 (*C*H), 124.4 (*C*H), 128.3 (*C*H), 128.5 (*C*H), 129.6 (*C*H), 131.9 (*C*H), 139.0, 143.6, 147.3 ppm. IR (ATR): $\tilde{\nu}$ = 3243, 3060, 3025, 2954, 2921, 2852, 2310, 1506, 1448, 1376, 1286, 1269, 1186, 1053, 994, 937, 903, 838, 824, 767, 744, 730, 607 cm^{-1}; HR-ESI-TOF-MS (positive mode): *m*/*z* calcd. for $C_{25}H_{22}ONa$: 361.1568, found: 361.1557 $[M+Na]^+$.

9-Ethynyl-9*H*-fluoren-9-yl octanoate (2a). The title compound **2a** was prepared according to a slightly modified literature procedures in which esterification was carried out after desilylation.[23] *n*-Octanoyl chloride (1.2 mL, 7.01 mmol) was slowly added to a solution of **1a** (1.17 g, 5.67 mmol) and *N*,*N*-dimethyl-4-aminopyridine (DMAP) (16.2 mg, 0.133 mmol) in CH_2Cl_2 (10 mL) and triethylamine (1.7 mL) at 0 ºC under argon. The mixture was allowed to warm up to room temperature and stirred for 2 h, after which it was poured into ice water (30 mL). The organic layer was separated, the aqueous layer was extracted with CH_2Cl_2 (2 × 10 mL), and the combined organic layers were dried over $MgSO_4$. The solvent was removed under reduced pressure and the residue was purified by silica-gel flash chromatography (amine-treated SiO_2: CH_2Cl_2/*n*-hexane 1:20) to afford **2a** (1.82 g, 97%). Yellow oil; R_f = 0.35 (amine-treated SiO_2; CH_2Cl_2/*n*-hexane 1:20); ^{1}H NMR (400 MHz, $CDCl_3$): δ 0.89 (t, *J* = 7.2 Hz, 3H; CH_3), 1.20–1.35 (m, 8H; CH_2), 1.58–1.65 (m, 2H; CH_2), 2.31 (t, *J* = 7.6 Hz, 2H; CH_2), 2.63 (s, 1H; C*H*), 7.35 (dd, *J* = 7.6, 1.2 Hz; Ar-*H*), 7.43 (dd, *J* = 7.6, 1.2 Hz; Ar-*H*), 7.64 (d, *J* = 7.6 Hz; Ar-*H*), 7.85 (d, *J* = 7.6 Hz; Ar-*H*) ppm; ^{13}C{^{1}H} NMR (100 MHz, $CDCl_3$): δ 14.1, 22.6, 24.9, 28.9, 29.0, 31.7, 34.8, 73.8, 78.7, 80.9, 120.1, 125.9, 128.5, 130.1, 140.0, 143.9, 172.1 ppm. The NMR data are in accord with the literature values.

9-(Hex-1-yn-1-yl)-9*H*-fluoren-9-yl acetate (2b). 1b (0.870 g, 3.32 mmol) was dissolved in pyridine (1.9 mL, 23.5 mmol) and acetic anhydride (3.5 mL, 20.1 mmol) under argon in an oven-dried two-necked round bottom flask. The

mixture was stirred for 48 h at room temperature, after which it was poured into aqueous K_2CO_3 (100 mL, 10% w/v) and extracted with CH_2Cl_2 (4 × 20 mL). The combined organic layers were dried over $MgSO_4$. The solvent was removed under reduced pressure and the residue was purified by silica-gel flash chromatography (amine-treated SiO_2; EtOAc/*n*-hexane 1:10) to afford **2b** (1.00 g, 99%). Viscous pale yellow solid; R_f = 0.38 (amine-treated SiO_2; EtOAc/*n*-hexane 1:10); m.p. 53–55ºC; ^{1}H NMR (400 MHz, $CDCl_3$): δ 0.84 (t, *J* = 7.4 Hz, 3H; C*H*$_3$), 1.33 (sext, *J* = 7.4 Hz, 2H; C*H*$_2$), 1.43 (quint, *J* = 7.4 Hz, 2H; C*H*$_2$), 1.96 (s, 3H; C*H*$_3$), 2.18 (t, *J* = 7.4 Hz, 2H; C*H*$_2$), 7.28 (dd, *J* = 7.6, 0.8 Hz, 2H; Ar-*H*), 7.33 (dd, *J* = 7.6, 0.8 Hz, 2H; Ar-*H*), 7.56 (d, *J* = 7.6 Hz, 2H; Ar-*H*), 7.80 (d, *J* = 7.6 Hz, 2H; Ar-*H*) ppm; ^{13}C{^{1}H} NMR (100 MHz, $CDCl_3$): δ 13.5 (*C*H$_3$), 18.5 (*C*H$_2$), 21.7 (*C*H$_3$), 21.7 (*C*H$_2$), 30.3 (*C*H$_2$), 77.0, 79.5, 86.7, 119.9 (*C*H), 125.7 (*C*H), 128.2 (*C*H), 129.6 (*C*H), 139.6, 144.7, 168.9 (*C*=O) ppm; IR (ATR): $\tilde{\nu}$ = 3063, 2962, 2930, 2866, 2241, 1740, 1449, 1365, 1317, 1289, 1223, 1174, 1141, 1090, 1013, 974, 927, 768, 757, 733, 682, 640, 603, 567 cm^{-1}; HR-ESI-TOF-MS (positive mode): *m*/*z* calcd. for $C_{21}H_{20}O_2Na$: 327.1361, found: 327.1365 [*M*+Na]$^+$.

9-((4-*n*-Butylphenyl)ethynyl)-9*H*-fluoren-9-yl acetate (2c). 1c (1.02 g, 3.01 mmol) was dissolved in pyridine (1.9 mL, 23.5 mmol) and acetic anhydride (3.5 mL, 20.1 mmol) under argon in an oven-dried two-necked round bottom flask. The mixture was stirred for 29 h at room temperature, after which it was poured into aqueous K_2CO_3 (100 mL, 10% w/v) and extracted with CH_2Cl_2 (4 × 20 mL). The combined organic layers were dried over Na_2SO_4. The solvent was removed under reduced pressure and the residue was purified by silica-gel flash chromatography (amine-treated SiO_2; EtOAc/*n*-hexane 1:7) to afford **2b** (0.999 g, 87%). Viscous pale yellow solid; R_f = 0.38 (amine-treated SiO_2; EtOAc/*n*-hexane 1:10); m.p. 77–78ºC; ^{1}H NMR (400 MHz, $CDCl_3$): δ 0.98 (t, *J* = 7.2 Hz, 3H; C*H*$_3$), 1.38 (sext, *J* =

7.4 Hz, 2H; CH_2), 1.62 (quint, J = 7.4 Hz, 2H; CH_2), 2.12 (s, 3H; CH_3), 2.63 (t, J = 7.4 Hz, 2H; CH_2), 7.15 (AA'BB', J = 8.0 Hz, 2H; Ar-H), 7.39–7.51 (m, 6H; Ar-H), 7.70 (d, J = 7.2 Hz, 2H; Ar-H), 8.02 (d, J = 7.2 Hz, 2H; Ar-H) ppm; ^{13}C{^{1}H} NMR (100 MHz, $CDCl_3$): δ 14.0 (CH$_3$), 21.9 (CH$_3$), 22.3 (CH$_2$), 33.3 (CH$_2$), 35.6 (CH$_2$), 79.8, 85.4, 85.8, 119.4, 120.1 (CH), 126.0 (CH), 128.3 (CH), 128.4 (CH), 129.9 (CH), 132.0 (CH), 139.9, 143.8, 144.4, 169.2 (C=O) ppm; IR (KBr): $\nu^{\sim}$ = 3057, 2954, 2926, 2867, 2848, 2231, 1748, 1505, 1449, 1365, 1288, 1225, 1206, 1057, 1011, 968, 955, 903, 776, 742, 649, 564 cm^{-1}; HR-ESI-TOF-MS (positive mode): m/z calcd. for $C_{27}H_{24}O_2K$: 419.1413, found: 419.1398 [M+K]$^+$.

Synthesis of fullerene–fluorene dyads *Z*-3a and *E*-3a. 2a (224 mg, 0.675 mmol) was dissolved in toluene (15 mL) under argon in an oven-dried two-necked flask, and degassed using three freeze–pump–thaw cycles under reduced pressures. Fullerene C_{60} (81.4 mg, 0.113 mmol) and $PtCl_2$ (9.2 mg, 0.034 mmol) were placed in a Pyrex tube under argon. The toluene solution of **2a** and additional dry toluene (66 mL) were added to the tube using a syringe. The mixture was heated at 80 ºC and the reaction was monitored by TLC and HPLC. After completion of the reaction, the mixture was passed through a cotton plug and the solvent was removed under reduced pressure. Purification and isolation was accomplished by silica-gel flash chromatography (SiO_2; toluene/n-hexane 1:3, 1:2, then 1:1) followed by preparative HPLC (Buckyprep ϕ20 × 250 mm; Cosmosil; Nacalai Tesque Inc., toluene/n-hexane 1:1, flow rate 9.9 mL min^{-1}) to give ***Z*-3a** (3.1 mg, 3%) and ***E*-3a** (30.2 mg, 25%) together with unreacted C_{60} (11.3 mg, 14%).

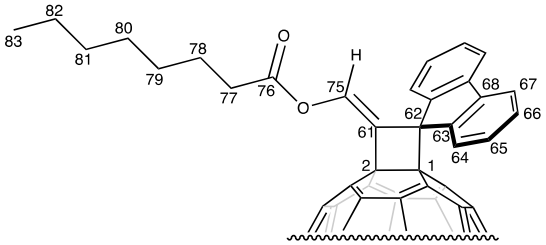

***Z*-3a:** Brown solid; R_f = 0.10 (SiO_2, toluene/n-hexane 1:3); ^{1}H NMR (400 MHz, $CDCl_3$): δ 0.84 (t, J = 7.2 Hz, 3H; CH_3), 1.15–1.30 (m, 8H; CH_2), 1.62 (quint, J = 7.5 Hz, 2H; CH_2), 2.43 (t, J

= 7.5 Hz, 2H; C*H*$_2$), 7.49–7.56 (m, 4H; Ar-*H*), 7.66 (s, 1H; C=C*H*), 7.85–7.88 (m, 2H; Ar-*H*), 8.47–8.51 (m, 2H; Ar-*H*) ppm; ^{13}C{^{1}H} NMR (100 MHz, $CDCl_3$): δ 14.25 (C83), 22.74 (*C*H$_2$), 24.80 (*C*H$_2$), 29.01 (*C*H$_2$), 29.11 (*C*H$_2$), 31.68 (*C*H$_2$), 34.23 (*C*H$_2$), 65.79 (C62), 70.54 (C2), 120.43 (C67), 127.49 (C64), 128.00 (C65 or C66), 129.01 (C66 or C65), 129.24, 134.75 (C75), 138.17, 138.35, 140.39, 140.97, 141.34, 141.64, 142.21, 142.26, 142.56, 142.82, 143.01, 143.18, 144.62, 144.74, 145.37, 145.41, 145.49, 145.52, 145.60, 146.02, 146.15, 146.22, 146.31, 146.62, 147.19, 147.22, 147.88, 151.03, 152.46, 169.84 (C76) ppm (45 resonances out of 49 expected ones due to peak overlap); λ_{max} = 438, 707 nm (in CS_2); ν(KCl)/cm^{-1} 3094, 3062, 3036, 2961, 2925, 2853, 1757, 1446, 1260, 1187, 1094, 1030, 800, 742, 526; MALDI-TOF MS (negative mode): *m*/*z* calcd. for $C_{83}H_{24}O_2$: 1052.178, found: 1052.178 [*M*]$^-$.

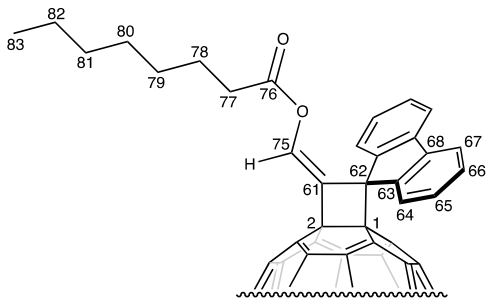

***E*-3a:** Brown solid; R_f = 0.15 (SiO_2, toluene/*n*-hexane 1:3); ^{1}H NMR (400 MHz, $CDCl_3$/CS_2 1:1): δ 0.91 (t, *J* = 7.2 Hz, 3H; C*H*$_3$), 0.96–1.21 (m, 8H; C*H*$_2$), 1.24–1.33 ((m, 2H; C*H*$_2$), 1.93 (t, *J* = 7.4 Hz, 2H; C*H*$_2$), 7.44–7.49 (m, 4H; Ar-*H*), 7.78–7.82 (m, 2H; Ar-*H*), 8.10 (s, 1H; C=C*H*), 8.39–8.44 (m, 2H; Ar-*H*) ppm; ^{13}C{^{1}H} NMR (100 MHz, $CDCl_3$/CS_2 1:1): δ 14.37 (C83), 22.98 (*C*H$_2$), 24.32 (*C*H$_2$), 28.94 (*C*H$_2$), 28.96 (*C*H$_2$), 31.78 (*C*H$_2$), 33.80 (*C*H$_2$), 66.13 (C62), 69.49 (C2), 76.09 (C1), 120.09 (C67), 127.04 (C64), 127.70 (C65 or C66), 128.65 (C66 or C65), 129.88 (C61), 134.31 (C75), 137.84, 138.37, 140.18, 140.96, 141.29, 141.42, 142.02, 142.12, 142.44, 142.69, 142.74, 142.83, 143.02, 144.47, 144.57, 145.16, 145.20, 145.29, 145.34, 145.52, 145.85, 145.94, 145.98, 146.06, 146.10, 146.54, 147.02, 147.06, 151.11, 152.66, 169.10 (*C*76) ppm (47 resonances out of 49 expected ones due to peak overlap); λ_{max} = 438, 709 nm (in CS_2); ν(KCl)/cm^{-1}

3066, 2921, 2848, 1751, 1690, 1446, 1198, 1129, 1104, 905, 741, 526; MALDI-TOF MS (negative mode): *m*/*z* calcd. for $C_{83}H_{24}O_2$: 1052.178, found: 1052.177 $[M]^-$.

Synthesis of Fullerene–fluorene dyad *Z*-3b. Fullerene C_{60} (81.2 mg, 0.113 mmol), **2b** (205.5 mg, 0.676 mmol), and $PtCl_2$ (9.3 mg, 0.035 mmol) were placed in a Pyrex tube under argon. Dry toluene (81 mL) was added to the tube using a syringe. The mixture was heated at 80 ºC and the reaction was monitored by TLC and HPLC. After completion of the reaction, the mixture was passed through a cotton plug and the solvent was removed under reduced pressure. Purification and isolation was accomplished by silica-gel flash chromatography (SiO_2; toluene/*n*-hexane 1:2) and subsequent preparative HPLC (Buckyprep ϕ20 × 250 mm; Cosmosil; Nacalai Tesque Inc., toluene/*n*-hexane 1:1, flow rate 9.9 mL min^{-1}) if required to give ***Z*-3b** (52.0 mg, 45%) together with unreacted C_{60} (26.8 mg, 33%).

***Z*-3b:** Brown solid; R_f = 0.28 (SiO_2, toluene/*n*-hexane 1:2); ^1H NMR (400 MHz, $CDCl_3/CS_2$ 1:1): δ 0.56 (t, *J* = 7.4 Hz, 3H; C*H*$_3$), 0.97 (sext, *J* = 7.4 Hz, 2H; C*H*$_2$), 1.18 (quint, *J* = 7.4 Hz, 2H; C*H*$_2$), 1.78 (t, *J* = 7.4 Hz, 2H; C*H*$_2$), 2.06 (s, 3H; C*H*$_3$), 7.45–7.54 (m, 4H; Ar-*H*), 7.79–7.83 (m, 2H; Ar-*H*), 8.47–8.51 (m, 2H; Ar-*H*) ppm; $^{13}C\{^1H\}$ NMR (100 MHz, $CDCl_3/CS_2$ 1:1): δ 13.65 (C79), 20.64 (C81), 22.32 (C78), 28.03 (C77), 29.46 (C76), 65.95 (C62), 70.66 (C1 or C2), 75.28 (C2 or C1), 120.25 (C67), 127.48 (C64), 127.87 (C65 or C66), 128.85 (C66 or C65), 129.56 (C61), 137.89, 138.25, 140.19, 140.74, 141.17, 141.44, 141.99, 142.11, 142.21, 142.43, 142.58, 142.64, 142.81, 143.03, 144.47, 144.53, 145.19, 145.34, 145.81, 145.92, 145.97, 146.06, 146.59, 146.98, 147.03, 150.68 (C75), 150.99, 152.20, 168.18 (C80) ppm (42 resonances out of 47 expected ones due to peak overlap); λ_{max} = 438, 708 nm (in CS_2); ν(KCl)/cm^{-1} 3059, 3016, 2959, 2937, 2858, 1759, 1715, 1462, 1447, 1427, 1366, 1199, 1181, 1165, 742, 526; MALDI-TOF MS

(negative mode): *m*/*z* calcd. for $C_{81}H_{20}O_2$: 1024.146, found: 1024.143 $[M]^-$.

Synthesis of Fullerene–fluorene dyad *Z*-3c. Fullerene C_{60} (81.1 mg, 0.113 mmol), **2c** (257.3 mg, 0.676 mmol), and $PtCl_2$ (9.2 mg, 0.035 mmol) were placed in a Pyrex tube under argon. Dry toluene (81 mL) was added to the tube using a syringe. The mixture was heated at 80 ºC and the reaction was monitored by TLC and HPLC. After completion of the reaction, the mixture was passed through a cotton plug and the solvent was removed under reduced pressure. Purification and isolation was accomplished by silica-gel flash chromatography (SiO_2; toluene/*n*-hexane 1:1) and subsequent preparative HPLC (Buckyprep ϕ20 × 250 mm; Cosmosil; Nacalai Tesque Inc., toluene/*n*-hexane 1:1, flow rate 9.9 mL min^{-1}) if required to give ***Z*-3c** (14.3 mg, 12%) together with unreacted C_{60} (67.1 mg, 83%).

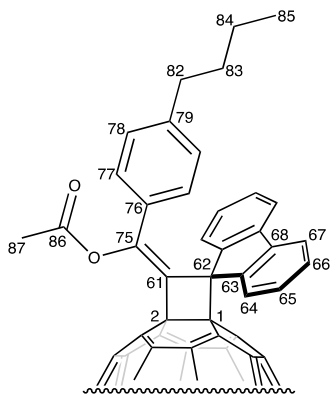

***Z*-3c:** Brown solid; R_f = 0.30 (SiO_2, toluene/*n*-hexane 1:1); ^{1}H NMR (400 MHz, $CDCl_3$): δ 0.87 (t, *J* = 7.4 Hz, 3H; C*H*$_3$), 1.20 (sext, *J* = 7.4 Hz, 2H; C*H*$_2$), 1.43 (quint, *J* = 7.4 Hz, 2H; C*H*$_2$), 2.19 (s, 3H; C*H*$_3$), 2.41 (t, *J* = 7.4 Hz, 2H; C*H*$_2$), 6.76 (AA'BB', *J* = 8.2 Hz, 2H; Ar-*H*), 6.82 (AA'BB', *J* = 8.2 Hz, 2H; Ar-*H*), 7.43–7.48 (m, 4H; Ar-*H*), 7.82–7.85 (m, 2H; Ar-*H*), 8.46–8.51 (m, 2H; Ar-*H*) ppm; ^{13}C{^{1}H} NMR (100 MHz, $CDCl_3$): δ 14.07 (C85), 21.13 (C87), 22.28 (C84), 33.27 (C83), 35.39 (C82), 67.43 (C62), 71.93 (C1 or C2), 75.67 (C2 or C1), 120.46 (C67), 126.11 (C77), 127.50 (C64), 127.97 (C65 or C66), 128.17 (C78), 128.93 (C66 or C65), 129.63 (C76), 131.25, 138.30, 138.44, 140.39, 140.81, 141.45, 141.64, 142.20, 142.30, 142.43, 142.56, 142.75, 142.82, 143.02, 143.21, 143.99 (C79), 144.68, 144.74, 145.41, 145.58, 146.03, 146.07, 146.16, 146.25, 146.29, 147.25, 147.29, 147.63 (C75), 151.37, 152.22, 169.11 (C86) ppm (46 resonances out of 51 expected ones due to peak overlap); λ_{max} = 433, 700 nm (in CS_2); ν(ATR)/cm^{-1} 3064, 2953, 2924, 2854, 1766, 1655, 1608, 1559, 1541, 1509,

1448, 1427, 1364, 1261, 1197, 1153, 1082, 1067, 1039, 895, 871, 801, 621, 597, 575, 562, 551; MALDI-TOF MS (negative mode): *m*/*z* calcd. for $C_{87}H_{24}O_2$: 1100.178, found: 1100.178 $[M]^-$.

X-ray crystallographic analysis of *Z*-3b. X-Ray diffraction (XRD) measurements were performed at 90 K on a Bruker AXS APEX III machine equipped with a Photon II detector with MoKα radiation (λ = 0.71073 Å). A specimen of $C_{81}H_{20}O_2$, approximate dimensions 0.060 mm × 0.269 mm × 0.284 mm, was used for the X-ray crystallographic analysis. The integration of the data using an orthorhombic unit cell yielded a total of 76675 reflections to a maximum θ angle of 27.10° (0.78 Å resolution), of which 9438 were independent (average redundancy 8.124, completeness = 99.7%, R_{int} = 6.04%, R_{sig} = 4.34%) and 6489 (68.75%) were greater than 2σ(F^2). The final cell constants of *a* = 19.3947(6) Å, *b* = 17.2114(5) Å, *c* = 25.7129(8) Å, volume = 8583.2(5) Å^3, are based upon the refinement of the XYZ-centroids of 9934 reflections above 20 σ(*I*). The calculated minimum and maximum transmission coefficients (based on crystal size) are 0.9740 and 0.9940. The structure was solved and refined using the Bruker SHELXTL Software Package, using the space group *Pbca*, with *Z* = 8 for the formula unit, $C_{81}H_{20}O_2$. The final anisotropic full-matrix least-squares refinement on F^2 with 769 variables converged at R_1 = 5.97%, for the observed data and wR_2 = 17.70% for all data. The goodness-of-fit was 1.054. The largest peak in the final difference electron density synthesis was 0.645 e^-/Å^3 and the largest hole was –0.628 e^-/Å^3 with an RMS deviation of 0.075 e^-/Å^3. On the basis of the final model, the calculated density was 1.586 g/cm^3 and F(000), 4176 e^-. CCDC 1887323 (***Z*-3b**) contains the supplementary crystallographic data for this paper. These data can be obtained free of charge from The Cambridge Crystallographic Data Centre via www.ccdc.cam.ac.uk/data_request/cif.

Thermal stability experiments

A solution of dyad **3** (3.3×10^{-4} M) and C_{70} (2.0×10^{-4} M) in toluene (100 μL) was placed in a Pyrex tube. After degassing through three freeze–pump–thaw cycles under reduced pressure, the tube was sealed and heated at 80ºC or 110 ºC for 1 h. The decomposition process was monitored by HPLC.

ASSOCIATED CONTENT

Supporting Information

Crystallographic data, HPLC chromatograms, mass spectra, IR spectra, absorption spectra, NMR spectra, electrochemical data, and computational results. The Supporting Information is available free of charge on the ACS Publications website.

AUTHOR INFORMATION

Corresponding Author

* E-mail: myamada@u-gakugei.ac.jp

NOTES

The authors declare no competing financial interest.

ACKNOWLEDGMENTS

This work was supported by the Japan Prize Foundation and TOBE MAKI Scholarship Foundation, and was partly supported by a Grant-in-Aid for Young Scientists (B) (16K17890) and a Grant-in-Aid for Scientific Research (B) (17H02735) from the Ministry of Education, Culture, Sports, Science, and Technology of Japan. The authors also thank Prof. Takashi Hirano of the University of Electro-Communications for performing ESI-TOF mass measurements.

REFERENCES

(1) *Modern Allene Chemistry, Volumes* 1–2; Krause, N.; Hashmi, S. K. Eds.; Wiley-VCH: Weinheim, 2004.

(2) (a) Krause, N.; Hoffmann-Röder, A. Synthesis of Allenes with Organometallic Reagents, *Tetrahedron* **2004**, *60*, 11671-11694. (b) Krause, N.; Winter, C. *Chem. Rev.* Gold-Catalyzed Nucleophilic Cyclization of Functionalized Allenes: A Powerful Access to Carbo- and Heterocycles, **2011**, *111*, 1994–2009.

(3) Yu, S.; Ma, S. Allenes in Catalytic Asymmetric Synthesis and Natural Product Syntheses, *Angew. Chem. Int. Ed.* **2012**, *51*, 3074-3112.

(4) Rivera-Fuentes, P.; Diederich, F. Allenes in Molecular Materials, *Angew. Chem. Int. Ed.* **2012**, *51*, 2818-2828.

(5) Nair, V.; Sethumadhavan, D.; Nair, S. M.; Shanmugam, P.; Treesa, P. M.; Eigendorf, G. K. Reaction of Allenamides with [60]Fullerene: Formation of Novel Cyclobutane Annulated Fullerene Derivatives, *Synthesis* **2002**, 1655-1657.

(6) Bildstein, B.; Schweiger, M.; Angleitner, H.; Kopacka, H.; Wurst, K.; Ongania, K.-H.; Fontani, M.; Zanello, P. Tetraferrocenyl[5]cumulene, $(Fc)_2C{=}C{=}C{=}C{=}C(Fc)_2$: Synthesis, Electrochemistry, and Reactivity, Including Nickel(0)-Promoted [3]Ferrocenophane Formation and [2+2] Cycloaddition with Fullerene C_{60}, *Organometallics* **1999**, *18*, 4286-4295.

(7) Ueda, M.; Sakaguchi, T.; Hayama, M.; Nakagawa, T.; Matsuo, Y.; Munechika, A.; Yoshida, S.; Yasuda, H.; Ryu, I. Regio- and Stereo-selective Intermolecular [2+2] Cycloaddition of Allenol Esters with C_{60} Leading to Alkylidenecyclobutane-Annulated Fullerenes, *Chem. Commun*. **2016**, *52*, 13175-13178.

(8) Yamada, M.; Ochi, R.; Yamamoto, Y.; Okada, S.; Maeda, Y. Transition-Metal-Catalyzed Divergent

Functionalization of [60]Fullerene with Propargylic Esters, *Org. Biomol. Chem.* **2017**, *15*, 8499-8503.

(9) (a) Buchmeiser, M.; Schotenberger, H. Ferrocenyl- and Ethynyl-Substituted Fluorenes via Addition-Elimination Reactions and Two-Electron Reductions from Fluorene. Syntheses of Heterodinuclear Acetylene and Fluorenyl Complexes, *Organometallics* **1993**, *12*, 2472-2477. (b) Banide, E. V.; Ortin, Y.; Seward, C. M.; Harrington, L. E.; Müller-Bunz, H.; McGlinchey, M. J. Sequential Formation of Yellow, Red, and Orange 1-Phenyl-3,3-Biphenylene-Allene Dimers Prior to Blue Tetracene Formation: Helicity Reversal in *trans*-3,4-Diphenyl-1,2-bis(fluorenylidene)cyclobutane, *Chem. Eur. J.* **2006**, *12*, 3275-3286. (c) Banide, E. V.; Molloy, B. C.; Ortin, Y.; Müller-Bunz, H.; McGlinchey, M. From Allenes to Tetracenes: A Synthetic and Stuctural Study of Silyl- and Halo-Allenes and Their Dimers, J. *Eur. J. Org. Chem.* **2007**, 2611-2622.

(10) Alcaide, B.; Almendros, P.; Aragoncillo, P. Exploiting [2+2] Cycloaddition Chemistry: Achievements with Allenes, *Chem. Soc. Rev.* **2010**, *39*, 783-816.

(11) Palomas, D.; Holle, S.; Inés, B.; Bruns, H.; Goddard, R.; Alcarazo, M. Synthesis and Reactivity of Electron Poor Allenes: Formation of Completely Organic Frustrated Lewis Pairs, *Dalton Trans.* **2012**, *41*, 9073-9082.

(12) Liou, K.-F.; Cheng, C.-H. Phosphine-Mediated [2+2] Cycloaddition of Internal Alk-2-ynoate and Alk-2-ynone to [60]Fullerene, *J. Chem. Soc., Chem. Commun.* **1995**, 2473-2474.

(13) Caporossi, F.; Floris, B.; Galloni, P.; Gatto, E.; Venanzi, M.; Mozzi, A. F.; Urbani, A.; Kadish, K. M. Fluorene-Fullerene Dyads: Modulation of Interaction, *Synth. Met.* **2009**, *159*, 1403-1408.

(14) Wolinski, K.; Hinton, J. F.; Pulay, P. Efficient Implementation of the Gauge-independent Atomic Orbital Method for NMR Chemical Shift Calculations, *J. Am. Chem. Soc.* **1990**, *112*, 8251-8260.

(15) The GIAO-B3LYP/6-31G(d) method has proven to be sufficiently accurate for reproducing the ^{1}H and ^{13}C NMR chemical shifts of fullerenes and fullerene derivatives: (a) Sun, G.; Kertesz, M. Theoretical ^{13}C NMR Spectra of IPR Isomers of Fullerenes C_{60}, C_{70}, C_{72}, C_{74}, C_{76}, and C_{78} Studied by Density Functional Theory, *J. Phys. Chem. A* **2000**, *104*, 7398-7403. (b) Duchamp, J. C.; Demortier, A.; Fletcher, K. R.; Dorn, D.; Iezzi, E. B.; Glass, T.; Dorn, H. C. An Isomer of the Endohedral Metallofullerene $Sc_3N@C_{80}$ with D_{5h} Symmetry, *Chem. Phys. Lett.* **2003**, *375*, 655-659. (c) Ref. 8.

(16) (a) Ishida, T.; Shinozuka, K.; Nogami, T.; Sasaki, S.; Iyoda, M. First X-Ray Structural Determination of Fullerene [2+2] Cycloadduct, *Chem. Lett.* **1995**, *4*, 317–318. (b) Wang, G.-W.; Komatsu, K.; Murata, Y.; Motoo, S. Synthesis and X-Ray Structure of Dumb-bell-shaped C_{120}, *Nature* **1997**, *387*, 583–586. (c) Fujiwara, K.; Komatsu, K. First Synthesis of a Highly Symmetrical Deckis-Adduct of Fullerene Dimer C_{120}, *Chem. Commun.* **2001**, 1986-1987. (d) Reboredo, S.; Girón, R. M.; Filippone, S.; Mikie, T.; Sakurai, T.; Seki, S.; Martín, N. Cyclobuteno[60]fullerenes as Efficient n-Type Organic Semiconductors, *Chem. Eur. J.* **2016**, *22*, 13627-13631.

(17) (a) Osterodt, J.; Nieger, M.; Vögtle, F. First X-Ray Determination of Cyclopropane Structure in Methanofullerenes, *J. Chem. Soc., Chem. Commun.* **1994**, 1607-1608. (b) Anderson, H. L.; Boudon, C.; Diederich, F.; Gisselbrecht, J.-P.; Gross, M.; Seiler, P. 61,61-Bis(trimethylsilylbutadiynyl)-1,2-dihydro-1,2-methanofullerene[60]: Crystal Structure at 100 K and Electrochemical Conversion to a Conducting Polymer, *Angew. Chem., Int. Ed. Engl.* **1994**, *33*, 1628-1632.

(18) (a) Rubin, Y.; Khan, S.; Freedberg, D. I.; Yeretzian, C. Synthesis and X-Ray Structure of a Diels-Alder Adduxt of Fullerene C_{60}, *J. Am. Chem. Soc.* **1993**, *115*, 344-345. (b) Khan, S. I.; Oliver, A. M.; Paddon-Row, M. N.; Rubin,

Y. Synthesis of a Rigid "Ball-and-Chain" Donor-Acceptor System through Diels-Alder Functionalization of Buckminsterfullerene (C_{60}), *J. Am. Chem. Soc.* **1993**, *115,* 4919-4920. (c) Diederich, F.; Jonas, U.; Gramlich, V.; Herrmann, A.; Ringsdorf, H.; Thilgen, C. Synthesis of a Fullerene Deriative of Benzo[18]crown-6 by *Diels-Alder* Reaction: Complexation Ability, Amphiphilic Properties, and X-Ray Crystal Structure of a Dimethoxy-1,9-(methano[1,2]benzenomethano)fullerene[60] Benzene Clathrate, *Helv. Chim. Acta* **1993**, *76*, 2445-2453. (d) Belik, P.; Gügel, A.; Kraus, A.; Spickermann, J.; Enkelmann, V.; Frank, G.; Müllen, K. The Diels-Alder Adduct of C_{60} and 4,5-Dimethoxy-*o*-quinodimethane–Synthesis, Crystal Structure, and Donor-Acceptor Behavior, *Adv. Mater.* **1993**, *5*. 854-856.

(19) (a) Sun, D.; Reed, C. A. Crystal Engineering a Linear Polymer of C_{60} Fullerene *via* Supramolecular Pre-Organization, *Chem. Commun.* **2000**, 2391-2392. (b) Zhong, Y.-W.; Matsuo, Y.; Nakamura, E. Lamellar Assembly of Conical Molecules Possessing a Fullerene Apex in Crystals and Liquid Crystals, *J. Am. Chem. Soc.* **2007**, *129*, 3052-3053. (c) Li, C.-Z.; Matsuo, Y.; Sato, Y.; Nakamura, E. Face-to-Face C_6F_5–[60]Fullerene Interaction for Ordering Fullerene Molecules and Application to Thin-Film Organic Photovoltaics, *Chem. Commun.* **2010**, *46*, 8582-8584. (d) Abe, Y.; Tanaka, H.; Guo, Y.; Matsuo, Y.; Nakamura, E. Mobility of Long-Lived Fullerene Radical in Solid State and Nonlinear Temperature Dependence, *J. Am. Chem. Soc.* **2014**, *136*, 3366-3369. (e) Umeyama, T.; Miyata, T.; Jakowetz, A. C.; Shibata, S.; Kurotobi, K.; Higashino, T.; Koganezawa, T.; Tsujimoto, M.; Gelinas, S.; Matsuda, W.; Friend, R. H.; Imahori, H. Regioisomer Effects of [70]Fullerene Mono-Adduct Acceptors in Bulk Heterojunction Polymer Solar Cells, *Chem. Sci.* **2017**, *8*, 181–188.

(20) Matsuda, T.; Kadowaki, S.; Goya, T.; Murakami, M. A Direct Entry to Bicyclic Cyclobutenes via Platinum-

Catalyzed Cycloisomerization of Allenynes, *Synlett* **2006**, 575–578.

(21) The $PtCl_2$-catalyzed reaction of C_{60} with **2b** was not affected by the protection from ambient light and by the presence of TEMPO (36 equiv. based on C_{60}), suggesting that both photoactivated species and free radical species are not involved in the reaction.

(22) Recent DFT calculations revealed that [2+2] cycloaddition of benzyne to C_{60} involves stepwise processes with the initial formation of a singly bonded diradical intermediate: Martínez, J. P.; Langa, F.; Bickelhaupt, F. M.; Osuna, S.; Solà, M. (4+2) and (2+2) Cycloadditions of Benzyne to C_{60} and Zig-Zag Single-Walled Carbon Nanotubes: The Effect of the Curvature, *J. Phys. Chem. C* **2016**, *120*, 1716-1726.

(23) Miki, K.; Senda, Y.; Kowada, T.; Ohe, K. Platinum- and Palladium-Catalyzed Sequential Reactions: Regioselective Synthesis of 9-Fluorenylidenes from 9-Ethynylfluoren-9-yl Carboxylates and Furans, *Synlett* **2009**, *12*, 1937-1940.

(24) (a) Miki, K.; Fujita, M.; Uemura, S.; Ohe, K. Ru-Catalyzed Ring-Opening and Substitution Reactions of Heteroaromatic Compounds Using Propargylic Carboxylates as Precursors of Vinylcarbenoids, *Org. Lett.* **2006**, *8*, 1741-1743. (b) Ikeda, Y.; Murai, M.; Abo, T.; Miki, K.; Ohe, K. Transition Metal-Catalyzed Ring-Opening, Substitution, and Cyclopropanation Reactions via Vinylcarbene Complexes Generated from *O*-Propargyl Thiocarbamates, *Tetrahedron Lett.* **2007**, *48*, 6651-6654.

(25) Yamada, M.; Akasaka, T.; Nagase, S. Carbene Additions to Fullerenes, *Chem. Rev.* **2013**, *113*, 7209-7264.

(26) (a) Merlic, C. A.; Bendorf, H. D. Cyclopropanation of C_{60} via a Fischer Carbene Complex. *Tetrahedron Lett.* **1994**, *35*, 9529-9532. (b) Bespalova, N. B.; Bovina, M. A.; Rebrov, A. I.; Sergeeva, M. B. Cyclopropanation of

Buckminsterfullerene *via* Olefin Metathesis Reaction, *Russ. Chem. Bull.* **1996**, *45*, 1255-1256. (c) Pellicciari, R.; Annibali, D.; Costantino, G.; Marinozzi, M.; Natalini, B. Dirhodium(II) Tetraacetate-Mediated Decomposition of Ethyldiazoacetate and Ethyldiazomalonate in the Presence of Fullerene. A New Procedure for the Selective Synthesis of [6-6]-Closed Methanofullerenes, *Synlett* **1997**, 1196-1198. (d) Roberti, M.; Natalini, B.; Andrisano, V.; Seraglia, R.; Gioiello, A.; Pellicciari, R. Thermal and Catalytic Reactions of Ethyl Diazopyruvate with [60]Fullerene, *Tetrahedron* **2010**, *66*, 7329-7332.

(27) Suzuki, T.; Maruyama, Y.; Akasaka, T.; Ando, W.; Kobayashi, K.; Nagase, S. Redox Properties of Organofullerenes, *J. Am. Chem. Soc.* **1994**, *116*, 1359-1363.

(28) Patiny, L.; Borel, A. ChemCalc: A Building Block for Tomorrow's Chemical Infrastructure, *J. Chem. Inf. Model.* **2013**, *53*, 1223-1228.

(29) Frisch, M. J.; Trucks, G. W.; Schlegel, H. B.; Scuseria, G. E.; Robb, M. A.; Cheeseman, J. R.; Scalmani, G.; Barone, V.; Mennucci, B.; Petersson, G. A.; Nakatsuji, H.; Caricato, M.; Li, X.; Hratchian, H. P.; Izmaylov, A. F.; Bloino, J.; Zheng, G.; Sonnenberg, J. L.; Hada, M.; Ehara, M.; Toyota, K.; Fukuda, R.; Hasegawa, J.; Ishida, M.; Nakajima, T.; Honda, Y.; Kitao, O.; Nakai, H.; Vreven, T.; Montgomery, J. A., Jr.; Peralta, J. E.; Ogliaro, F.; Bearpark, M.; Heyd, J. J.; Brothers, E.; Kudin, K. N.; Staroverov, V. N.; Kobayashi, R.; Normand, J.; Raghavachari, K.; Rendell, A. J.; Burant, C.; Iyengar, S. S.; Tomasi, J.; Cossi, M.; Rega, N.; Millam, J. M.; Klene, M.; Knox, J. E.; Cross, J. B.; Bakken, V.; Adamo, C.; Jaramillo, J.; Gomperts, R.; Stratmann, R. E.; Yazyev, O.; Austin, A. J.; Cammi, R.; Pomelli, C.; Ochterski, J. W.; Martin, R. L.; Morokuma, K.; Zakrzewski, V. G.; Voth, G. A.; Salvador, P.; Dannenberg, J. J.; Dapprich, S.; Daniels, A. D.; Farkas, O.; Foresman, J. B.; Ortiz, J. V.; Cioslowski, J.; Fox, D. J.

Gaussian 09, revision D.01; Gaussian, Inc.: Wallingford, CT, 2013.

(30) (a) Becke, A. D. Density-Functional Exchange-Energy Approximation with Correct Asymptotit Behavior, *Phys. Rev. A* **1988**, *38*, 3098-3100. (b) Becke, A. D. Density-Functional Thermochemistry. III. The Role of Exact Exchange, *J. Chem. Phys.* **1993**, *98*, 5648-5652. (c) Lee, C.; Yang, W.; Parr, R. G. Development of the Colle-Salvetti Correlation-Energy Formula into a Functional of the Electron Density, *Phys. Rev. B* **1988**, *37*, 785-789. (d) Hehre, W. J.; Ditchfield, R.; Pople, J. A. Self-Consistent Molecular Orbital Methods. XII. Further Extensions of Gaussian-Type Basis Sets for Use in Molecular Orbital Studies of Organic Molecules, *J. Chem. Phys.,* **1972**, *56*, 2257-2261.

(31) (a) Hennion, G. F.; Fleck, B. R. Reactions of Some Aromatic Acetylenic Carbinols, *J. Am. Chem. Soc.* **1955**, *77*, 3253–3258. (b) Chiarucci, M.; Syntrivanis, L.-D.; Cera, G.; Mazzanti, A.; Bandini, M. Merging Synthesis and Enantioselective Functionalization of Indoles by a Gold-Catalyzed Asymmetric Cascade Reaction, *Angew. Chem. Int. Ed.* **2013**, *52*, 10850-10853. (c) Hosseinzadeh, R.; Abolfazli, M. K.; Mohseni, M.; Mohadjerani, M.; Lasemi, Z. Efficient Synthesis and Antibacterial Activities of Some Novel 1,2,3-Triazoles Prepared from Propargylic Alcohols and Benzyl Azides, *J. Heterocyclic Chem.* **2014**, *51*, 1298-1305.

(32) Zhang, H.; Tanimoto, H.; Morimoto, T.; Nishiyama, Y.; Kakiuchi, K. Regioselective Rapid Synthesis of Fully Substituted 1,2,3-Triazoles Mediated by Propargyl Cations, *Org. Lett.* **2013**, *15*, 5222-5225.

Table of Contents

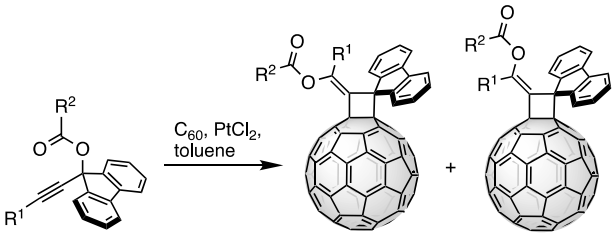

Single-step regio- and stereoselective reactions

Crystal structure of an alkylidenecyclobutane-annulated fullerene featuring close-packed arrays of C_{60} spheres